EULERIAN SIMULATION OF INTERACTING PWR SPRAYS INCLUDING DROPLET COLLISIONS

KEYWORDS: *containment, spray, collision*

A. FOISSAC,[a] J. MALET,[a]* S. MIMOUNI,[b] P. RUYER,[a] F. FEUILLEBOIS,[c] and O. SIMONIN[d]

[a]*Institut de Radioprotection et de Sureté Nucléaire, Saclay, France*
[b]*Electricité de France, Chatou, France*
[c]*Laboratoire d'Informatique pour la Mécanique et les Sciences de l'Ingénieur Orsay, France*
[d]*Institut de Mécanique des Fluides de Toulouse, Toulouse, France*

A numerical simulation of the interaction between two real pressurized water reactor containment sprays is performed with a new model implemented into the Eulerian computational fluid dynamics (CFD) code NEPTUNE_CFD. The water droplet polydispersion in size has been treated with a sectional approach. The influence of collisions between droplets is taken into account with a statistical approach based on the various outcomes of binary collision. Experiments were performed in a new facility, and data obtained are compared with this two-fluid simulation. The results show good agreement.

I. INTRODUCTION

Spray systems are emergency devices designed for preserving the containment integrity in case of a severe accident in a pressurized water reactor (PWR). These systems are used to prevent overpressure, to cool the containment atmosphere, to remove fission products from the containment atmosphere, and to enhance the gas mixing in case of the presence of hydrogen in the reactor containment. The efficiency of these sprays can depend partially on the evolution of the droplet size distribution in the containment, due to gravity and drag forces; heat and mass transfers with the surrounding gas; and droplet collisions. Spray systems in nuclear power plants are composed of more than 500 interacting water droplet sprays with droplet diameters ranging from 100 to 1000 μm. They are used under pressure (2 to 3 bars) at temperatures between 20°C and 60°C and under a gaseous mixture composed of steam, hydrogen, and air.

Droplet interactions are generally neglected in safety codes because of the lack of accurate industrial modeling of such sophisticated physics. However, studying droplet interactions in the field of spray systems in nuclear reactor containment is clearly justified since more than 500 spray nozzles that are either oriented downward or inclined are used in a PWR, resulting in an overlap of the spray envelopes.[1]

Few experiments exist in the field of interacting sprays,[2–4] and they are performed on sprays that do not have the same ranges of parameters (droplet sizes and velocities, as well as distance between sprays) as the ones used in a PWR. A specific experimental facility, presented in this paper, has thus been built in order to study the configuration of two PWR interacting sprays.

Considering computational fluid dynamics (CFD) studies on spray interactions, one can find different approaches in the literature.[5] Since our work uses a code having a Eulerian approach for droplet transport, the Lagrangian approach for polydispersed flow and collisions is not considered here. For the Eulerian droplet approach, two main groups of methods describe the polydispersion of particles: the sectional method[6–8] and the method of moments.[9,10] PWR sprays are characterized by high relative velocities between droplets. The sectional method

*E-mail: jeanne.malet@irsn.fr

is the most appropriate method to take into account the various trajectories of droplets depending on their diameter. Therefore, the sectional method is used here.

In the literature a collision kernel has already been introduced into polydispersed flows of droplets. In the past studies, as soon as the droplets collide, only two issues have been considered: bouncing or coalescence. However, the literature has shown that binary droplet collision can have a wider range of issues, such as separation into three droplets or splashing into tiny drops.[11–14] Preliminary estimations have shown that the splashing regime could occur for droplets of two interacting PWR sprays.[14] Thus, we propose here to implement a complete "collision issue" on the basis of the modeling of binary collision.[13]

The objective of this work is thus to present our model for droplet collision numerical simulations and to compare the results with the data obtained on experiments specifically developed for this study, based on two interacting real PWR sprays.

II. PWR CONTAINMENT SPRAY SYSTEMS

The French PWR containments (Fig. 1) have generally two series of nozzles placed in circular rows. More precisely, for the 900-MW(electric) PWR, there are exactly four rings of nozzles having the characteristics presented in Table I. A schematic view of these spray rings and the associated spray envelopes are given in Fig. 1. The nozzle type used in many PWRs, in particular, French 900-MW(electric) PWRs, is the so-called SPRACO 1713A, distributed by Lechler under reference 373.084.17.BN (Fig. 1). This nozzle is generally used with water at a relative pressure of 350 kPa, producing a flow rate of ~1 ℓ/s. The outlet orifice diameter is 9.5 mm. The temperature of the injected water during a hypothetical nuclear reactor accident is either from 20°C or 60°C to 100°C, depending on the kind of process (the 60°C to 100°C process is the so-called recirculation mode).

TABLE I

Characteristics of Spray Rings for the French 900-MW(electric) PWR

	Height (m)	Diameter (m)	Number of Nozzles	Approximated Distance Between Nozzles (m)
First ring	54.8	10.0	66	0.5
Second ring	54.2	14.8	68	0.7
Third ring	52.3	22.5	186	0.4
Fourth ring	51.0	27.0	186	0.4

III. EXPERIMENTAL MEASUREMENT OF PWR CONTAINMENT SPRAY CHARACTERISTICS

III.A. CALIST Facility

Experiments have been carried out at the French Institut de Radioprotection et Sûreté Nucléaire (IRSN), on

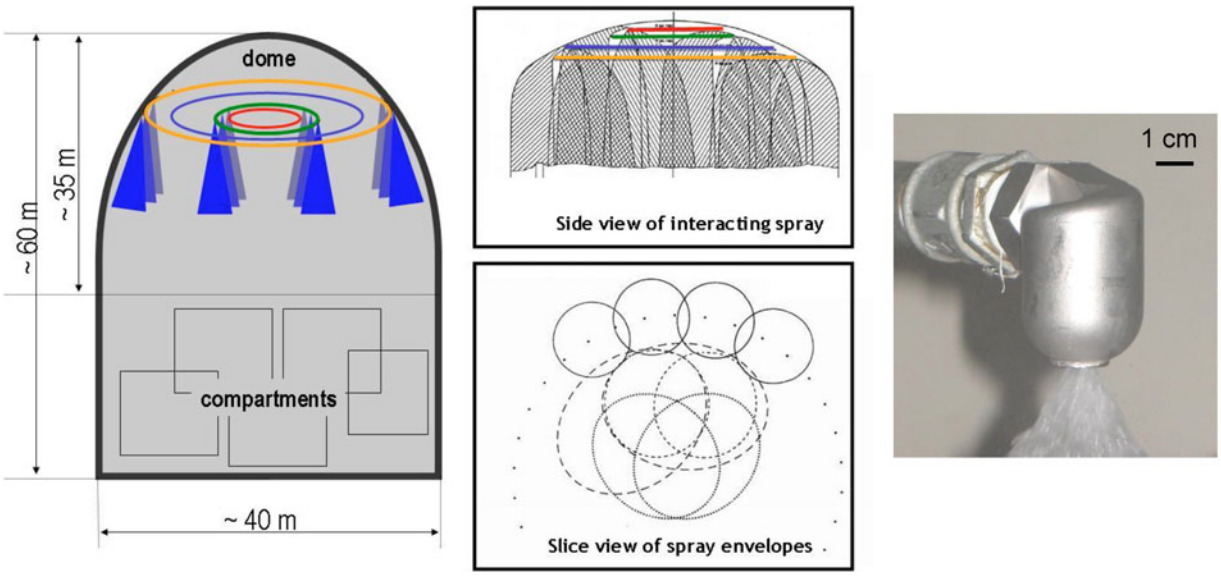

Fig. 1. Spray rings and envelopes in a French PWR (not at scale) and spray nozzle SPRACO 1713A (Lechler 373.084.17.BN).

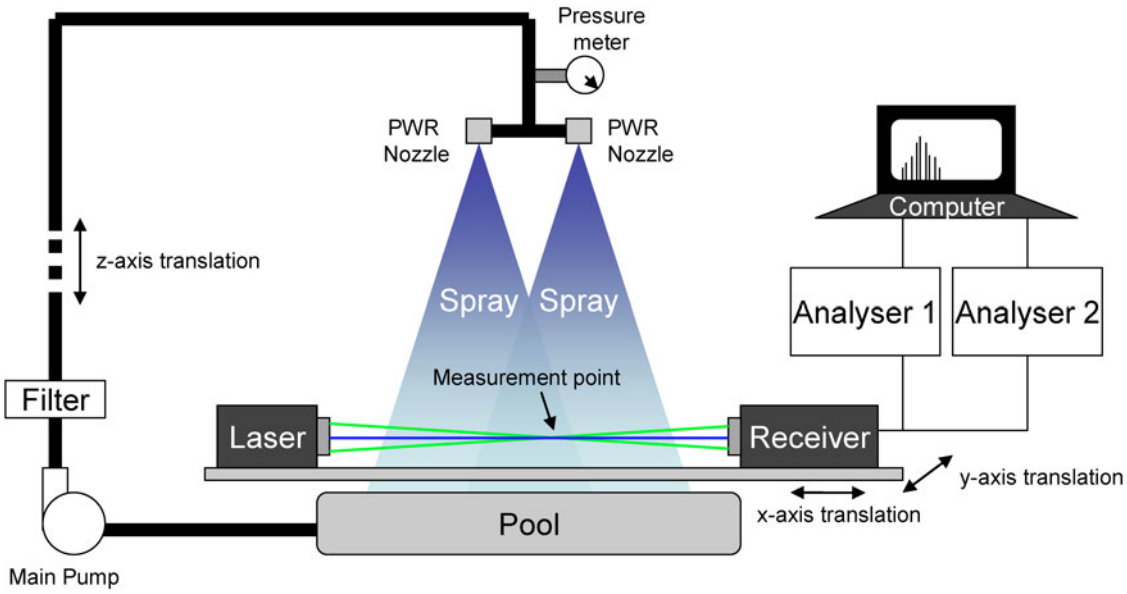

Fig. 2. CALIST water-spray experimental facility.

the CALIST (Characterization and Application of Large and Industrial Spray Transfer) facility sketched in Fig. 2. In a room of 7- × 6- × 3.5-m^3 dimensions, the setup is composed of a water-supplying hydraulic circuit and, for these experiments, two interacting spray nozzles with a flow rate of 1 ℓ/s at a relative pressure of 350 kPa for each nozzle and separated by 42 cm. The water spray, with a temperature of ~15°C to 20°C, is collected in a 5-m^3 pool. The axial position of the spray nozzle may be changed using a monitored carriage.

The measurement of the spray characteristics requires a technique such as light diffraction, shadowgraphy, or phase Doppler interferometry (PDI). The latter is chosen since it provides local high-resolution information about the spray drops. Indeed, PDI measures the size and the velocity of drops passing through an optically defined probe volume.[15]

PDI can measure only droplets of spherical shape. In order to determine where atomization is achieved—and, so, when droplets are spherical—visualization is performed with a Phantom high-speed camera used with a resolution of 800 × 600 pixels at a frequency of 4796 Hz, with an exposure time of 10 μs (Ref. 16). The spray is illuminated from the back in order to obtain consistent and machine-readable images. The high-speed visualization shows that the distance from the nozzle exit at which most of the liquid is atomized into droplets is ~20 cm. Therefore, it can be anticipated that at such a distance, PDI measurements of droplets are reliable. Measurements have been performed at 20, 40, 60, and 80 cm from the nozzle exit.

The uncertainty of the measurement radial positions is due to the spray specific oscillations at the considered pressure supply of this spray nozzle. These oscillations were clearly attributed to the spray and not to any system, such as the water pump. They are estimated to be ~1 cm.

The uncertainty of the droplet variables is calculated from three uncertainties: (a) the uncertainty based on measurement repeatability (measurements are generally repeated at least three times); (b) the uncertainty based on the angular position (measurements performed at four angular positions, in a spray that has been found to be axisymmetric[16]); and (c) the uncertainty based on the already mentioned spray oscillations (the uncertainty of the measurement position introduces an uncertainty of the droplet variable measurement: This uncertainty is thus calculated by estimating the variation of the variable over the radial position).

An example of the good repeatability of the tests is presented in Fig. 3.

III.B. Characteristics of Droplets 20 cm from the Nozzle

Measurements performed 20 cm from the nozzles are used as inlet conditions of the numerical simulations. At this distance, because of the hollow cone created by these nozzles, most of the droplets are concentrated in an annular area located between 8 and 15 cm from the nozzle axis, with a maximum of presence at 11 cm, as can be seen in Fig. 4a, where the local water concentration is normalized by its maximum value. The geometric mean diameter D_{10}, Sauter mean diameter D_{32}, and mean velocities are displayed in Fig. 4b as functions of the distance from the nozzle axis. D_{10} varies between ~240 and 330 μm. D_{32} varies between 360 and 520 μm. This implies dispersion in size. The axial velocity v_z is maximum

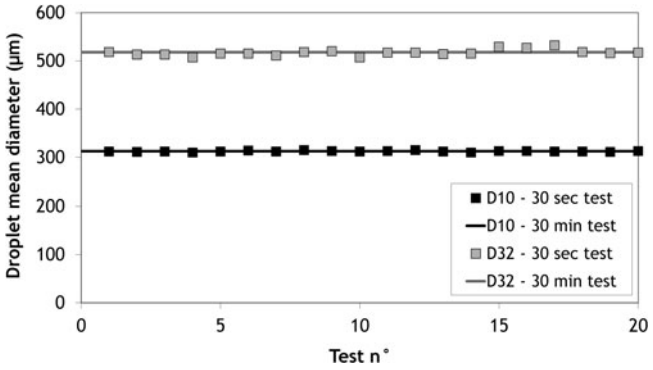

Fig. 3. Repeatability study on droplet size measurements.

close to the nozzle axis: It is 20 m/s at 8 cm and then decreases radially to 13 m/s at 15 cm. The radial velocity v_r is maximal far from the nozzle axis and equal to 7.7 m/s. The orthoradial velocity v_θ is very low and varies between 0.17 and 0.34 m/s. This means that the swirl created by the nozzle internal geometry is attenuated very quickly in the first centimeters when atomization occurs.

Figure 5 shows the local spray size and axial velocity distributions (normalized by their maximal values). One can see that the shape of the size distribution does not depend on the distance from the nozzle axis. The size distribution can be approximated with a lognormal law as presented by Ref. 16.

IV. MODELING OF DROPLET POLYDISPERSION AND COLLISIONS

Numerical simulations have been performed using the NEPTUNE_CFD code.[17] The solver belongs to the well-known class of pressure-based methods. It is able to simulate multicomponent multiphase flows by solving a set of three balance equations for each field (fluid

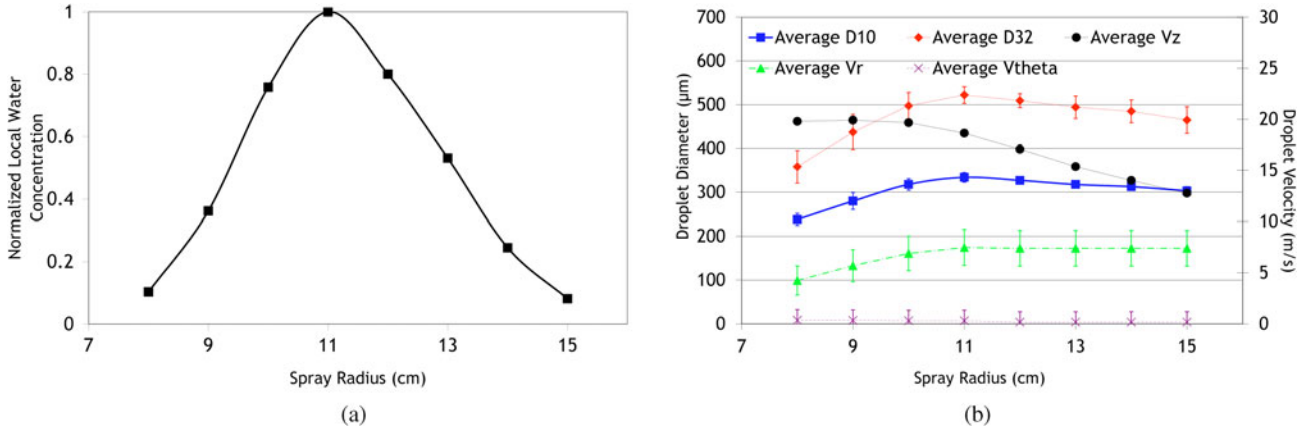

Fig. 4. Mean characteristics of the spray 20 cm from the nozzle outlet (error bars are given for a 67% interval of confidence).

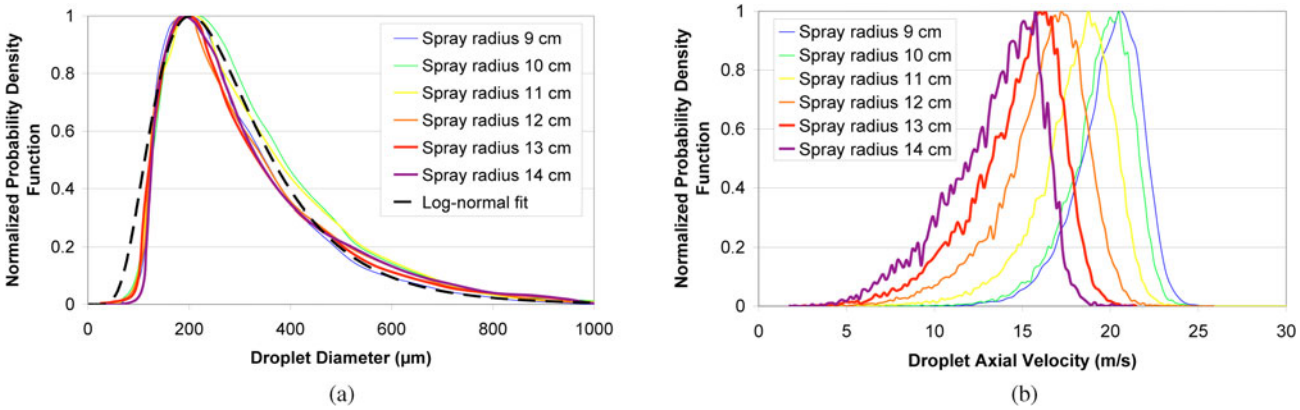

Fig. 5. Experimental size and axial velocity distributions 20 cm from the nozzle, presented for different distances from the nozzle axis.

component and/or phase). These fields can represent many kinds of multiphase flows: distinct physical components (e.g., gas, liquid, and solid particles); thermodynamic phases of the same component (e.g., liquid water and its vapor); distinct physical components, some of which split into different groups (e.g., water and several groups of different-diameter bubbles); and different forms of the same physical components (e.g., a continuous liquid field, a dispersed liquid field, a continuous vapor field, and a dispersed vapor field). The solver is implemented in the NEPTUNE software environment, which is based on a finite volume discretization, together with a collocated arrangement for all variables. The data structure is totally face based, which allows the use of arbitrarily shaped cells (tetrahedra, hexahedra, prisms, pyramids, etc.) including no conforming meshes. The main interest of the numerical method is the so-called "volume fraction–pressure–energy cycle," which ensures mass and energy conservation and allows strong interface source-term coupling. In the simulations described later, gas turbulence is associated with the $k-\varepsilon$ model, whereas dispersed phase turbulence is modeled with the Q2-Q12 model.[18] For the latter, for each droplet class, the turbulent kinetic energy equation is based on the same turbulent kinetic energy equation as the one used for the gas phase, with a contribution coming from all forces due to the presence of all other droplet classes. Closure laws are also derived from the correlation between gas and droplet fluctuations, leading to a transport equation of this variable based on the Ref. 19 approach, modified by Ref. 18. In this transport equation, the turbulent dynamic viscosity between the gas and the droplets depends on a droplet gas entrainment characteristic time, derived by Ref. 20, and simplified by Ref. 21. In this paper, focus is given on the collision model, which is described in this section.

IV.A. Modeling of Droplet Polydispersion

Reference 6 develops a method to model particle polydispersion in size in Eulerian simulations. The idea is to consider the dispersed phase as a set of continuous "fluid" media: each fluid corresponding to a statistical average between two fixed droplet sizes, namely, a section. The spray is then described by a set of conservation equations for each fluid. In our case, both interacting sprays will be considered as independent fluids, and for each spray or fluid, size distributions are divided into sections of fixed diameter. Sections are chosen as fixed in size, and they exchange mass and momentum in order to model evaporation/condensation or collision phenomena.

IV.B. Mass Balance Equations

The several-fluids model consists of a mass balance equation, where k represents each section and i is the coordinate:

$$\frac{\partial}{\partial t}(\alpha_k \rho_k) + \frac{\partial}{\partial x_i}(\alpha_k \rho_k U_{k,i}) = \Gamma_k^{collision} + \Gamma_k^{cond/evap} \quad , \tag{1}$$

where

t = time

$\alpha_k, \rho_k, U_{k,i}$ = void fraction of section k, its averaged density, and its velocity along the coordinate i, respectively

$\Gamma_k^{collision}, \Gamma_k^{cond/evap}$ = mass transfer per unit volume and unit time due to collisions and condensation/evaporation, respectively.

It is assumed that no evaporation or condensation occurs in this case: $\Gamma_k^{cond/evap} = 0$.

$\Gamma_k^{collision}$ consists of a source term Γ_k^{coll+} and a sink term Γ_k^{coll-}:

$$\Gamma_k^{collision} = \Gamma_k^{coll+} + \Gamma_k^{coll-} \quad . \tag{2}$$

It can be written that

$$\begin{cases} \Gamma_k^{coll+} = \displaystyle\sum_{m,n} \Gamma_{m,n\to k} \quad , \\ \Gamma_k^{coll-} = -\displaystyle\sum_{m,n} \Gamma_{k,m\to n} \quad , \end{cases} \tag{3}$$

where $\Gamma_{m,n\to k}$ is the mass transfer from section m to k after a collision between droplets of class m and droplets of class n.

IV.C. Momentum Balance Equations

The momentum balance equation is given by

$$\begin{aligned} &\frac{\partial}{\partial t}(\alpha_k \rho_k U_{k,i}) + \frac{\partial}{\partial x_j}(\alpha_k \rho_k U_{k,i} U_{k,j}) \\ &\quad = -\alpha_k \nabla p + \alpha_k \rho_k g + \nabla[\alpha_k(\tau_k + \tau_k^T)] \\ &\qquad + \sum_{m,n} \Gamma_{m,n\to k}(U_{m,n\to k,i} - U_{k,i}) \quad , \end{aligned} \tag{4}$$

where

p = pressure

g = gravity

τ_k, τ_k^T = molecular and turbulent stress tensors (Reynolds stress tensor)

$U_{m,n\to k,i}$ = velocity of section k along coordinate i resulting from the collision between droplets of class m and droplets of class n.

IV.D. Mass Transfer Terms due to Collision

$\Gamma_k^{collision}$ can be derived from two terms: Γ_k^{coll+} as a positive term (creation of droplets of class k) and a negative term Γ_k^{coll-} (sink of droplets of class k) due to collisions. The positive term can be expressed as

$$\Gamma_k^{coll+} = \sum_{m,n} \alpha_m \rho_m f_{m,n} [Coll^{m,n}\, prob^{m,n}(\mathrm{We}_s)] \ , \quad (5)$$

where

We_s = symmetric Weber number of the collision

$f_{m,n}$ = collision frequency between droplets of class m and n, described in Sec. III.F

$prob^{m,n}$ = matrix of probabilities to obtain a given collision issue regime at the related Weber number described in Sec. III.G

$Coll^{m,n}$ = so-called outcome collision matrix of each regime, described in more detail in Ref. 22.

The negative term Γ_k^{coll-} is described in the same way as the production term, but the outcome collision matrix is different.[22]

IV.E. Momentum Transfer Term due to Collision

The momentum transfer term due to collision is obtained on the same basis as for mass transfer:

$$\Gamma_k (U_i^* - U_{k,i}) = \sum_{m,n} \alpha_m \rho_m f_{m,n} (U_{m,n\to k,i} - U_{k,i}) \, [Coll^{m,n}\, prob^{m,n}(\mathrm{We}_s)] \ . \quad (6)$$

The U_i^* velocity is the resulting velocity from the collision issue.

IV.F. Collision Frequency Equation

The collision frequency $f_{m,n}$ between droplets from sections m and n is derived from Ref. 23 as follows:

$$f_{m,n} = g_0^{mn} \pi \left(\frac{d_m + d_n}{2} \right)^2 n_n n_m |U_m - U_n| \times \left[\left(\frac{1}{2z} + 1 \right) \mathrm{erf}(\sqrt{z}) + \frac{\exp(-z)}{\sqrt{\pi z}} \right]$$

$$\text{with } z = \frac{3}{4} \frac{(U_m - U_n)^2}{q_m^2 + q_n^2 - 2\sqrt{q_m^2 q_n^2}\,\xi_m \xi_n} \ , \quad (7)$$

where

d_m, d_n = diameter of sections m and n, respectively

n_m, n_n = number concentration of sections m and n, respectively

q_m^2, q_n^2 = droplet kinetic energy at sections m and n, respectively

ξ_m, ξ_n = fluid-droplet velocity correlation coefficient of droplets of sections m and n, respectively

g_0 = radial distribution function introduced by Ref. 24:

$$g_0^{mn} = \left(1 - \frac{\sum_{p=m,n} \alpha_p}{0.64} \right)^{-0.64\gamma_{mn}}$$

$$\text{with } \gamma_{mn} = 1 + \frac{3}{2} \left(\frac{d_m d_n}{d_m + d_n} \right) \frac{2 \sum_{p=m,n} \alpha_p / d_p}{\sum_{p=m,n} \alpha_p} \ . \quad (8)$$

IV.G. Modeling of Collision Issues

Five binary collision outcome regimes can be pointed out: bouncing, coalescence, reflexive separation, stretching separation, and splashing.[14] Looking at the collision pictures,[25] one may possibly determine the final daughter diameter and velocity as a function of the initial "parent" diameters, using mass and momentum conservation. These values are summarized in Table II. For the splashing regime, a value of 20 droplets has been estimated, but this should be considered as a first approximation. All these collision issues can be represented by functions depending on the Weber number and the impact parameter of the collision, described hereinafter.

Reference 13 proposes simple formulas expressing the boundaries of collision outcome fields as a function of the symmetric Weber number expressed by

$$\mathrm{We} = \frac{\rho}{12\sigma} \frac{d_s^3 \|\vec{u}_s\|^2 + d_l^3 \|\vec{u}_l\|^2}{d_s^2 + d_l^2} \ . \quad (9)$$

In our calculations, the expressions of Ref. 13 for collision are used.

The critical impact parameter $I_c^{ref\text{-}coal}$ at which the transition between reflexive separation and coalescence occurs is given by

$$I_c^{ref\text{-}coal} = 0.28 \sqrt{1 - \frac{0.45}{\mathrm{We}}} \ . \quad (10)$$

The critical impact parameter $I_c^{stre\text{-}coal}$ for the transition between coalescence and stretching separation is expressed by

$$I_c^{stre\text{-}coal} = \frac{\sqrt{\mathrm{We}_{stre}^2 + 8\mathrm{We}_{stre}\mathrm{We}} - \mathrm{We}_{stre}}{4\mathrm{We}}$$

$$\text{with } \mathrm{We}_{stre} = 0.53 \ . \quad (11)$$

TABLE II

Daughter Droplet Diameters of Two Parents' Droplets After a Binary Collision for Different Regimes

Collision Outcome	Observations of Binary Collision Issues	Number of Formed Droplets in the Calculation	Final Droplet Diameter in the Calculation	Final Droplet Velocity in the Calculation
Bouncing	No change	Two	d_m and d_n	$\vec{U}_m$ and $\vec{U}_n$
Coalescence	Creation of one droplet	One	$\sqrt[3]{d_m^3 + d_n^3}$	$\frac{d_m^3 \vec{U}_m + d_n^3 \vec{U}_n}{d_m^3 + d_n^3}$
Stretching separation	Satellite droplets are neglected.	Two	d_m and d_n	$\vec{U}_m$ and $\vec{U}_n$
Reflexive separation	Three droplets are created.	Three	$\sqrt[3]{\frac{d_m^3 + d_n^3}{3}}$	$\frac{d_m^3 \vec{U}_m + d_n^3 \vec{U}_n}{d_m^3 + d_n^3}$
Splashing	Twenty droplets are created.	Twenty	$d_k = \sqrt[3]{\frac{d_m^3 + d_n^3}{20}}$	$\vec{U}_k$

The critical impact parameter $I_c^{ref\text{-}stre}$ between reflexion and stretching is given by

$$I_c^{ref\text{-}stre} = \sqrt{\frac{1-k}{1+R_{ref/stre}}} \tag{12}$$

with k a viscous dissipation coefficient, found experimentally in Ref. 13 to be equal to 0.9 and with dimensionless number $R_{ref/stre}$ that is found to be 0.28 according to experimental results.[13] Equations (10), (11), and (12) for the critical impact parameter, which describe the transition curves between collision regimes, are described in more detail in Ref. 13. They are valid under ambient gas conditions for droplet sizes between 200 and 400 μm, with velocities up to 10 $\mathrm{m \cdot s^{-1}}$. Where the transition to bouncing is concerned, the calculations performed here are based on the Ref. 12 model, described by Eq. (13):

$$\mathrm{We}_{coal/boun} = \frac{\Delta(1+\Delta^2)(4\Phi_c - 12)}{\chi(1-I^2)}$$

$$\text{with } \Phi_c = \frac{2}{\left(\frac{3}{\varphi_c^2}+1\right)^{2/3}} + \left(\frac{3}{\varphi_c^2}+1\right)^{1/3}, \tag{13}$$

where χ is the fraction of volume interaction and Δ is the diameter ratio. The parameter φ_c has to be obtained experimentally. Reference 21 performs binary water droplet collision experiments on the bouncing regime and finds the value for φ_c should be 0.3.

Concerning the fifth collision regime, the splashing regime (collision of two drops leads to the splashing into tiny droplets) is assumed to occur when the symmetrical Weber number is >20, based on experimental observations,[20] which have to be confirmed by further experiments. The model proposed here for splashing is a first approximation basic threshold model.

When these collision outcome equations are used, the probability $prob^{m,n}(\mathrm{We}_s)$ to obtain a given collision issue regime $\boldsymbol{p}$ at the related Weber number is obtained from the probability of the impact parameter, which follows a sinusoidal law described in detail in Ref. 22. This sinusoidal law results from the study of particle collisions whose trajectories are not correlated.

V. NUMERICAL SIMULATIONS OF SPRAYS

Before performing the simulations on two interacting PWR sprays, we validate simplified cases.

V.A. Validation of Polydispersity and Collision Models on a Simple Case

Reference 10 performs direct numerical simulations (DNSs) of particle clouds in homogeneous isotropic turbulence, without gravity. Simulations are conducted with an initially lognormal distributed droplet phase, in a cubical domain with 128^3 grid regular points for a cube physical length of 0.128 m and with periodical boundary conditions. An overview of the physical properties is given in Table III.

Figure 6 shows the size distribution evolution at different times, normalized on the initial distribution. One can notice that results from the sectional method described previously, used with nine sections in the NEPTUNE_CFD code, are quite similar to the DNS results. As a consequence, the sectional method and the polydispersity modeling are validated in the case of homogeneous isotropic turbulence. Further elementary simulations should be performed to validate the drift part of the collision frequency[10] since this is the main

TABLE III

Properties of Fluid and Initially Lognormal Distributed Droplet Phase*

Fluid Density	Fluid Kinematic Viscosity	Fluid Kinetic Energy, q^2_{fluid}
1.17 kg/m^3	1.47×10^{-5} m^2/s	0.0015 m^2/s^2

Droplet Void Fraction	Lognormal Mean Diameter	Lognormal Standard Deviation	Droplet Density	$q^2_{droplet}/q^2_{fluid}$
4.388×10^{-4}	260 μm	0.12	226.3 kg/m^3	0.890

*Reference 10.

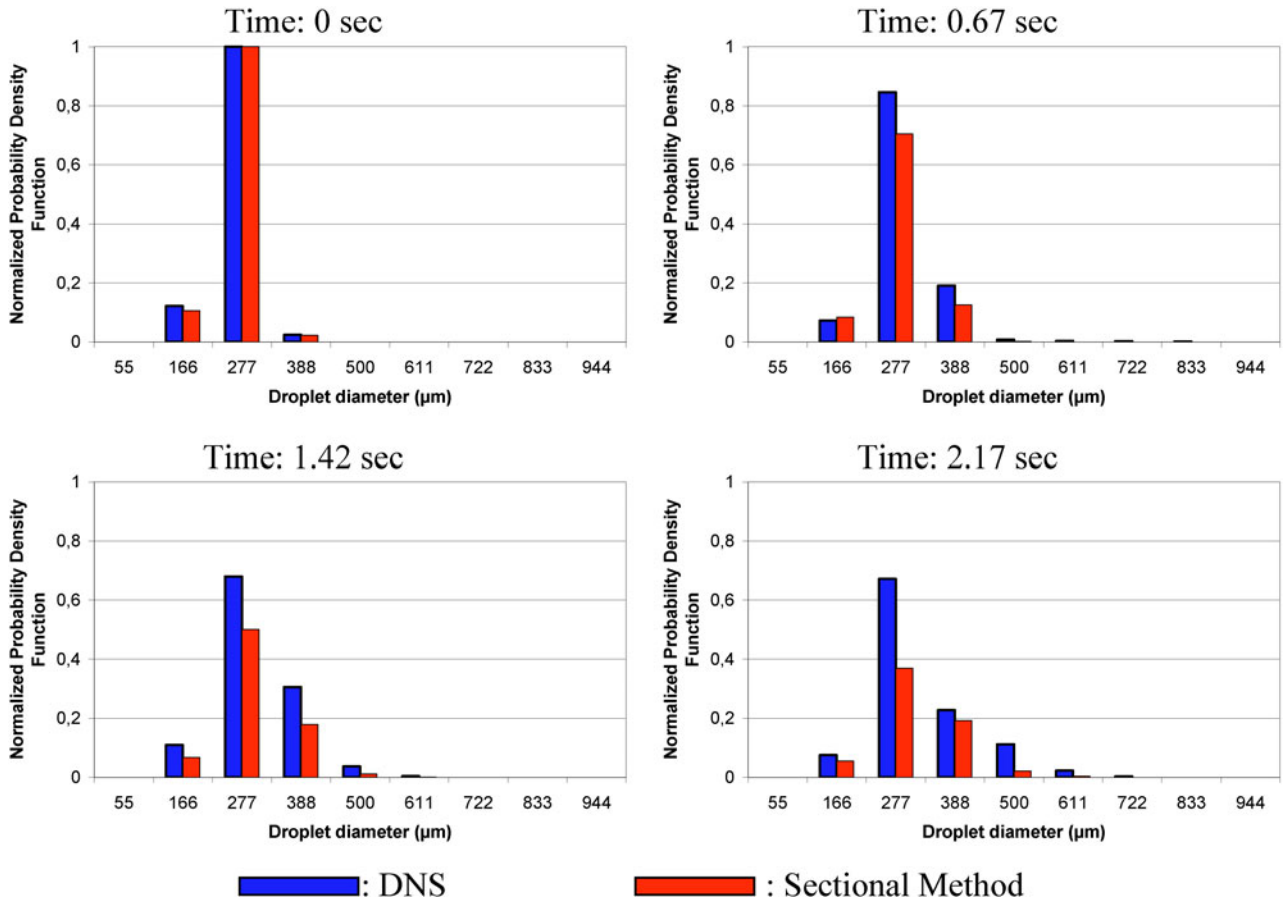

Fig. 6. Droplet size distribution evolution in time, comparison of DNS (Ref. 10) and present sectional method.

phenomenon responsible for the collision in the top of the reactor containment.

V.B. Numerical Simulation of Two PWR Interacting Sprays

Interacting sprays, characterized in the CALIST facility, are simulated inside a parallelepiped mesh of 800 000 hexahedra regular cells, representing a domain of $1.20 \times 0.80 \times 2$ m. All boundaries are considered as free outputs, except the top face, which contains the input and walls around, with no friction, and where velocity can only be tangential. Since the spray produced by these nozzles is a hollow cone extending 20 cm from the nozzle, the input domain is modeled by two annular rings of 18-cm internal diameter and 26-cm external diameter. Droplets are injected from this annular ring with the size distribution presented in Fig. 4. In Fig. 4, one can see that

the axial velocity decreases from 20 to 15 m/s with the distance to the nozzle axis.

In these simulations, we assumed that the injection velocity is independent of the position. We chose a value of 18.6 m/s, that is, the velocity 11 cm from the nozzle axis, where the volumetric fraction is maximal. Estimating the value of one single radial velocity for the simulation is more difficult. Indeed, this value is very important since it is the main component of the relative velocity of the droplets when the spray interacts and thus can modify the value of the Weber number and the collision efficiency. A value of 7.7 m/s was chosen according to the results presented in Fig. 3. The orthoradial velocity was neglected because of its low value. Each spray size distribution was separated into nine sections (Fig. 7), whose void fractions were adjusted from the assumed droplet size distribution in order to obtain a mass flow rate of 1 kg/s, as measured on the real PWR nozzle for a relative pressure of 3.5 bars.

The experimental and numerical local size distributions obtained are compared in Fig. 8 for different positions along the symmetrical axis. Code-experiment comparison leads to very encouraging results. The same overall size distribution is obtained in the experiment and in the calculations.

It is clear that the droplet size decreases since the mean geometric diameter is $\sim$300 μm before spray interaction and $\sim$200 μm after spray interaction (Fig. 8). This decrease can have two origins. First, it can be due to collisions at high Weber number that occur when sprays interact: In the interaction area, the collision frequency reaches a maximum of $\sim 10^{11}$ collisions$\cdot m^{-3} \cdot s^{-1}$, and the Weber number is very high, so that collisions could lead to breakup.[20] This size decrease is also due to the entrainment of the smallest droplets in the direction of the symmetrical axis.[26] The smallest droplets are drifted away in the air flow, whereas the biggest droplets, having more inertia, are not altered in the spray interacting area.

At this stage, it is difficult to explain the main phenomenon occurring because initial conditions and boundary conditions play a significant role. Calculations presented here have been performed with constant radial and axial velocity profiles. The difference between calculations using one single mean velocity compared to calculations using a real velocity profile has been recently investigated with one single spray simulation, as described in Ref. 27, indicating that further calculations of the interacting sprays using the exact experimental velocity profiles could be performed in the future to improve the numerical results.

Thus, for the sake of caution, it is preferred to test many parameters to evaluate their influence. Future work will thus be performed on the impact of the radial velocity at the inlet since it is involved in many critical parameters like the Weber number and the collision frequency. The sensitivity to the mesh or the choice of intervals of the size distribution are also issues for future work.

VI. CONCLUSION

A numerical simulation of the interaction between two PWR containment sprays has been performed with a new model of polydispersion and collision of droplets implemented into the Eulerian CFD code NEPTUNE_CFD. The droplet size and velocity distributions at a distance of 20 cm below the spray nozzle outlet have been precisely measured and used as input data in the calculations. The water droplet polydispersion in size has been treated with a sectional approach. The influence of collisions between droplets is taken into account with a statistical approach based on the various outcomes of binary collisions.

An elementary validation of one part of the collision model is performed, and our results are in good agreement with the DNS calculations. A two-fluid

Section	Diameter (μm)	Flowrate (kg/s)
1	55	$1.22\ 10^{-5}$
2	166	$6.28\ 10^{-3}$
3	277	$3.18\ 10^{-2}$
4	388	$7.31\ 10^{-2}$
5	500	$1.17\ 10^{-1}$
6	611	$1.56\ 10^{-1}$
7	722	$1.86\ 10^{-1}$
8	833	$2.07\ 10^{-1}$
9	944	$2.22\ 10^{-1}$

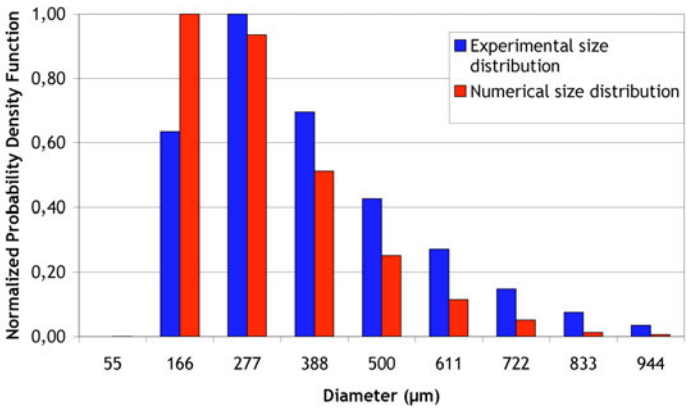

Fig. 7. Sections used for the numerical simulation, associated with the experimental size distribution to the location 20 cm from the nozzle.

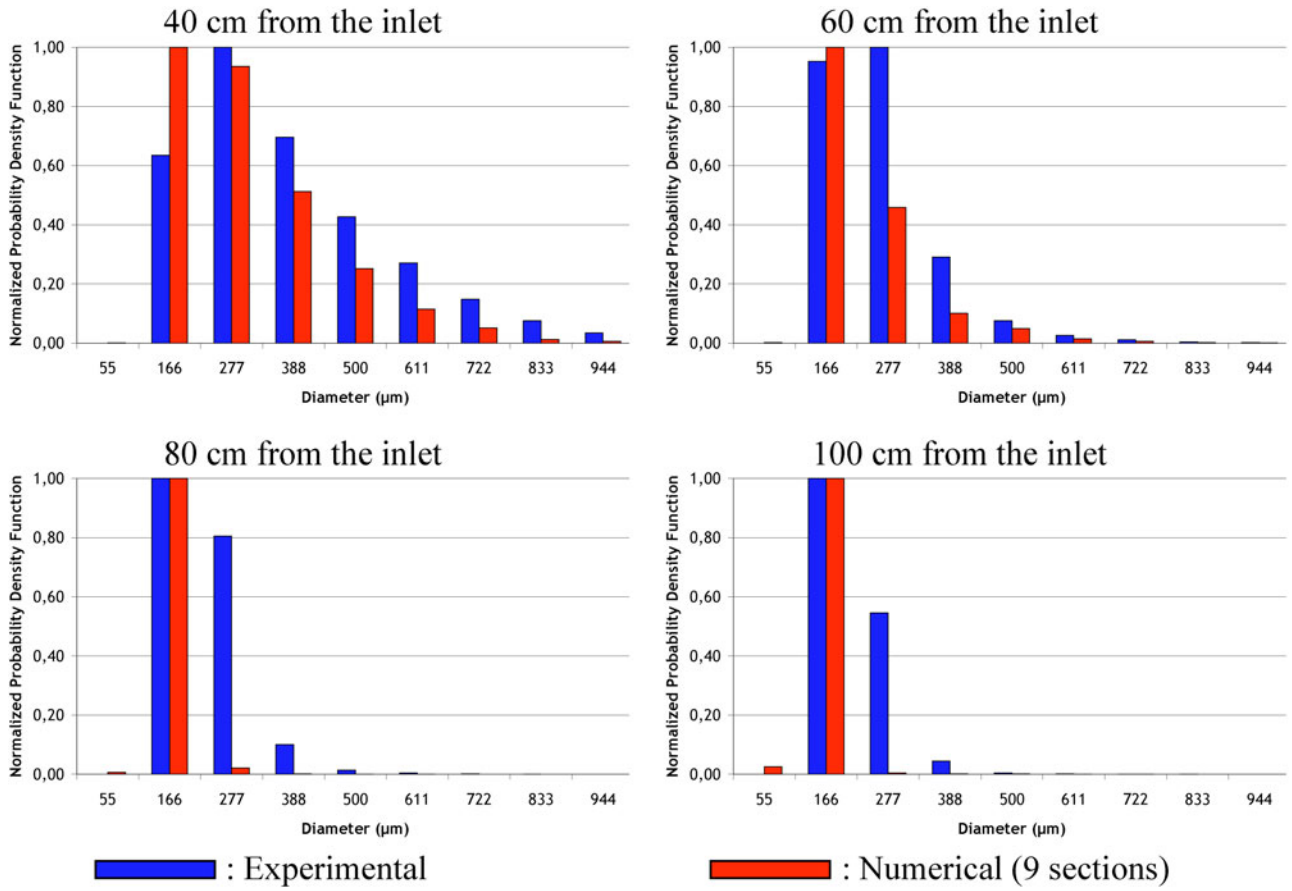

Fig. 8. Comparison between experimental and numerical size distributions on the symmetrical axis and for different distances from the inlet.

multidimensional simulation, based on two interacting real PWR spray nozzles, is compared to the results obtained in the CALIST facility and shows good agreement. These first results allow us to continue sensitivity studies in order to evaluate the most important phenomena involved in the droplet characteristics' evolution (condensation, evaporation, entrainment, and collision). For this purpose, more elementary simulations are however still needed. The impact of boundary conditions of the droplet characteristics has to be evaluated, as well as the validation of the gas entrainment by one single PWR spray assuming the simplified boundary conditions generally used in nuclear reactor simulations (one single droplet size and initial velocity characterize the spray).

For these purposes, an experiment to characterize the gas entrainment by a single PWR spray has been performed in the CALIST facility. These results allowed evaluation of the ability of codes to simulate the gas entrainment produced by a PWR spray and were proposed for benchmarking activities within the European Network of Excellence SARNET-2 (Ref. 28). Knowledge of these characteristics could be important to evaluate the efficiency of these spray systems in terms of depressurization, hydrogen mixing, and radioactive aerosol scavenging for applications concerning nuclear reactor accidents.

REFERENCES

1. C. RABE, J. MALET, and F. FEUILLEBOIS, "On the Influence of Droplet Coalescence in Spray Systems for Containment Safety," *Proc. 13th Int. Topl. Mtg. Nuclear Reactor Thermal Hydraulics (NURETH-13)*, Kanazawa City, Japan, September 27–October 2, 2009.

2. M. ARAI and M. SAITO, "Atomization Characteristics of Jet-to-Jet and Spray-to-Spray Impingement Systems," *Atom. Sprays*, **9**, 399 (1999).

3. T. CHIBA et al., "Inter-Spray Impingement of Two Diesel Sprays," *Proc. Int. Conf. Liquid Atomization and Spray Systems (ICLASS)*, Pasadena, California, July 16–20, 2000.

4. G. H. KO and H. S. RYOU, "Droplet Collision Processes in an Inter-Spray Impingement System," *J. Aerosol Sci.*, **36**, 1300 (2005).

5. A. A. MOSTAFA and H. C. MONGIA, "On the Modelling of Turbulent Evaporating Sprays: Eulerian Versus Lagrangian Approaches," *Int. J. Heat Mass Transfer*, **30**, 2583 (1987).

6. J. B. GREENBERG, I. SILVERMAN, and Y. TAMBOUR, "On the Origin of Spray Sectional Conservation Equations," *Combustion Flame*, **93**, 90 (1993).

7. F. LAURENT, M. MASSOT, and P. VILLEDIEU, "Eulerian Multi-Fluid Modeling for the Numerical Simulation of Coalescence in Polydisperse Dense Liquid Sprays," *J. Comput. Phys.*, **194**, 505 (2004).

8. P. VILLEDIEU and J. HYLKEMA, "Une méthode particulaire aléatoire reposant sur une équation cinétique pour la simulation numérique des sprays denses de gouttelettes liquides," *Comptes Rendus de l'Académie des Sciences de Paris*, **325**, Série I, 323 (1997).

9. R. O. FOX, F. LAURENT, and M. MASSOT, "Numerical Simulation of Spray Coalescence in an Eulerian Framework: Direct Quadrature Method of Moments and Multi-Fluid Method," *J. Comput. Phys.*, **227**, 3058 (2008).

10. D. WUNSCH, "Theoretical and Numerical Study of Collision and Coalescence—Statistical Modeling Approaches in Gas-Droplet Turbulent Flows," PhD Thesis, University of Toulouse (2010).

11. N. ASHGRIZ and J. Y. POO, "Coalescence and Separation in Binary Collisions of Liquid Drops," *J. Fluids Mech.*, **221**, 183 (1990).

12. J. P. ESTRADE, "Experimental Investigation of Dynamic Binary Collision of Ethanol Droplets—A Model for Droplet Coalescence and Bouncing," *Int. J. Heat Fluid Flow*, **20**, 486 (1999).

13. C. RABE, J. MALET, and F. FEUILLEBOIS, "Experimental Investigation of Water Droplet Binary Collisions and Description of Outcomes with a Symmetric Weber Number," *Phys. Fluids*, **22**, 047101 (2010).

14. N. ROTH et al., "Droplet Collision Outcomes at HighWeber Number," *Proc. 21st Conf. Institute for Liquid Atomization and Spray Systems (ILASS)*, Mugla, Turkey, September 10–12, 2007.

15. W. D. BACHALO and M. J. HOUSER, "Phase Doppler Spray Analyzer for Simultaneous Measurements of Drop Size and Velocity Distributions," *Opt. Eng.*, **23**, 583 (1984).

16. A. FOISSAC et al., "Droplet Size and Velocity Measurements at the Outlet of a Hollow-Cone Spray Nozzle," *Atom. Sprays*, **21**, 893 (2011).

17. S. MIMOUNI et al., "Modelling of Sprays in Containment Applications with a CMFD Code," *Nucl. Eng. Des.*, **240**, *9*, 2260 (2010).

18. O. SIMONIN, "Combustion and Turbulence in Two-Phase Flows," von Karman Institute for Fluid Dynamics, Lecture Series, 1996–2002 (1996).

19. L. I. ZAICHIK, O. SIMONIN, and V. M. ALIPCHENKOV, "Two Statistical Models for Predicting Collision Rates of Inertial Particles in Homogeneous Isotropic Turbulence," *Phys. Fluids*, **15**, 2995 (2003).

20. O. SIMONIN, "Prediction of the Dispersed Phase Turbulence in Particle-Laden Jets," *Proc. 4th Int. Symp. Gas-Solid Flows*, ASME FED, Vol. 121, p. 197, ASME Fluids Engineering Division (1991).

21. J. POZORSKI and J. P. MINIER, "Probability Density Function Modelling of Dispersed Two-Phase Turbulent Flows," *Phys. Rev. E*, **59**, 855 (1999).

22. A. FOISSAC, "Modélisation des interactions entre gouttes en environnement hostile," PhD Thesis, University of Paris VI (2011).

23. F. PIGEONNEAU and F. FEUILLEBOIS, "Collision and Size Evolution of Drops in Homogeneous Isotropic Turbulence," *J. Aerosol Sci.*, **49**, S1279 (1998).

24. G. PATINO-PALACIOS and O. SIMONIN, "General Derivation of Eulerian-Eulerian Equations for Multiphase Flows," Institut de Mécanique des Fluides Toulouse (2003).

25. A. FOISSAC et al., "Binary Water Droplet Collision Study in Presence of Solid Aerosols in Air," *Proc. 7th Int. Conf. Multiphase Flow (ICMF)*, Tampa, Florida, May 30–June 4, 2010.

26. G. E. COSSALI, "An Integral Model for Gas Entrainment into Full Cone Sprays," *J. Fluids Mech.*, **439**, 353 (2001).

27. J. MALET et al., "Numerical Study on the Influence of Simplified Spray Boundary Conditions for the Characterisation of Large Industrial Safety Spray Systems Used in Nuclear Reactors," *Proc. Int. Conf. Atomication and Spray Systems (ICLASS 2012)*, Heidelberg, Germany, September 2–6, 2012.

28. J. MALET et al., "Gas Entrainment by One Single French PWR Spray, SARNET-2 Spray Benchmark," *Proc. 15th Int. Topl. Mtg. Nuclear Reactor Thermalhydraulics (NURETH-15)*, Pisa, Italy, May 12–16, 2013 (submitted for publication).